

## Article

# Synthesis and Application of a Low Dye Absorption Waterborne Polyurethane for Microfiber Synthetic Leather

Wenyu Cai , Wei Xin, Haonan Zhang and Yunjun Luo \* 

School of Materials Science and Engineering, Beijing Institute of Technology, Beijing 100081, China; cwy9051@163.com (W.C.); xinwii@126.com (W.X.); 18701120979@163.com (H.Z.)

\* Correspondence: yjluo@bit.edu.cn

**Abstract:** As increasing attention is being paid to harmful residual dye pollution in the dyeing effluent from the microfiber synthetic leather industry, there is an urgent need to explore innovative ways to alleviate such pollution. Here, a low-polarity waterborne polyurethane (WPU) was synthesized using hydroxyl-terminated polybutadiene (HTPB) and polypropylene glycol (N220) as soft segments to react with –NCO on isophorone diisocyanate (IPDI). The structure and properties of modified waterborne polyurethane were characterized by Fourier Transform Interferometric Radiometer (FTIR), and emulsion characterization was performed, including particle size and zeta potential analysis, tensile test, thermal properties test, and contact angle test. The SEM and alkali reduction rate results showed that increasing the HTPB content decreases the alkali reduction rate by blocking the penetration of corrosive ions by the double bond cross-link structure, but higher HTPB addition (>40%) leads to an enhancement in phase separation, which contributes to an increase in the alkali reduction rate. The results of the UV spectrum analysis showed that when the amount of HTPB added was 50%, the coloration rate reached 81.27% compared with 13.18%, which was 68.09% higher than that of the unmodified microfiber leather. The binding of the dry and wet rubbing color of the modified microfiber leather with the addition of 50% HTPB reached grades of 4–5 and 3–4, respectively, which meets most application requirements without subsequent washing.

**Keywords:** waterborne polyurethane; non-polar modification; microfiber synthetic leather; wash efficiency; dispersed dye



**Citation:** Cai, W.; Xin, W.; Zhang, H.; Luo, Y. Synthesis and Application of a Low Dye Absorption Waterborne Polyurethane for Microfiber Synthetic Leather. *Coatings* **2022**, *12*, 728. <https://doi.org/10.3390/coatings12060728>

Academic Editor: Joseph L. Keddie

Received: 25 April 2022

Accepted: 23 May 2022

Published: 25 May 2022

**Publisher's Note:** MDPI stays neutral with regard to jurisdictional claims in published maps and institutional affiliations.



**Copyright:** © 2022 by the authors. Licensee MDPI, Basel, Switzerland. This article is an open access article distributed under the terms and conditions of the Creative Commons Attribution (CC BY) license (<https://creativecommons.org/licenses/by/4.0/>).

## 1. Introduction

Microfiber synthetic leather is the third generation of artificial leather products. It is a 3D structure made of microfiber non-woven fabric as a substrate structure and polyurethane elastomer as a network structure, which plays the role of a filler. Because of this combined structure, microfiber leather has excellent thermodynamic, elasticity, and softness properties [1,2]. In the process of making microfiber leather, impregnation and alkali reduction are the two most important processes. The waterborne polyurethane is finally impregnated into the microfiber by pressing and rolling. Through the adhesion of polyurethane, the base fabric forms an organic overall structure and has a texture similar to leather [3,4]. The effect of the impregnation process directly determines the style, feel, elasticity, and mechanical properties of the synthetic microfiber leather.

Environmental pollution caused by waste dye is still a major challenge faced by the microfiber leather industry. During the dyeing stage, polyurethane easily absorbs dye, but later in the washing process, the dye attached to the polyurethane is also easily washed off but difficult to clean [5]. As a result, after dyeing, synthetic leather requires clean water for many washes, which causes serious environmental pollution [6].

Traditional waterborne polyurethanes are usually synthesized by the reaction of polyols and isocyanates. In addition, various chain extender structures are added, such as 1, 4-butanediol (BDO), and ethylenediamine (EDA). The polyols form the soft segment,

and the urethane bonds and urea bonds generated by the reaction of the diisocyanate and the chain extender form the hard segment; these segments are connected to each other by intermolecular forces and hydrogen bonds [7–11].

In recent years, polyurethane has been widely used in the field of perovskite solar cells. As a semiconductor material, perovskite cells are considered to be one of the most promising solar cells due to their excellent optoelectronic properties. Hot melt film materials used to encapsulate solar cells generally include three categories: polyurethane, PU; polyolefin, POE; and ethylene vinyl acetate, EVA. For perovskite solar cells, POE and EVA are not suitable for packaging due to the high packaging temperature and corrosion of perovskite absorbers. For thermosetting PU, it has the characteristics of good thermal stability, excellent chemical inertness, resistance to corrosion, and strong mechanical properties, so it is often used as an encapsulation for perovskite solar cells [12,13].

WPU can also be used as a leather finishing agent to improve the mechanical properties of leather and its antifouling properties. Wu et al. synthesized dihydroxyterminated 1,1,2,2-tetrahydroperfluorodecyl methacrylate (FDMA(OH)<sub>2</sub>) using a thiol-ene “click” reaction. Then, it was used as a chain extender for a OCN-terminated WPU to obtain fluorinated waterborne polyurethane (FWPU), which greatly improved the hydrophobicity and water-repellent and anti-fouling properties of WPU [14]. Liu et al. synthesized poly(propylene glycol) terminated with ortho-amiomethylphenyl diboronic acid (AMPBA-PPG) and cross-linked polymer containing boroxine (CLP-boroxine) using nucleophilic substitution. As a result, the dynamic reversible covalent bonds in AMPBA-PPG improved the self-healing efficiency of leather while the self-healing efficiency of the 15 wt% CLP-boroxine/WPU film was as high as 93.6% after only 4 h [15].

Waterborne polyurethane plays an important role in environmentally friendly modified materials. By introducing tannic acid (TA) into waterborne polyurethane, Luo et al. enhanced the polymer degradation ability and TA-modified WPU emulsion also showed an excellent comprehensive performance in the leather finishing experiment [16]. Compared with traditional solvent-based coatings, water-based coatings use water as the dispersed phase in the synthesis and production process, thus greatly reducing the amount of solvent used in the synthesis process and achieving the goal of green production. Traditional solvent-based polyurethane usually uses a large amount of acetone or butanone as the dispersion medium, and its cost is much higher than that of pure water, which leads to the cost of solvent-based polyurethane in the production process being much higher than that of water-based polyurethane. In addition, most traditional organic solvents are toxic, and indiscriminate discharge causes damage to humans through the environment [6,17–19].

Hydroxy-terminated polybutadiene (HTPB) has a non-polar hydrophobic carbon chain, double bonds, and a hydroxyl-terminated structure. The glass transition temperature in thermodynamics is relatively low, and the mechanical properties at low temperatures are excellent [18,20,21]. The synthesized waterborne polyurethane often exhibits strong mechanical properties, wear resistance, and low temperature flexibility and is often used in the field of adhesives and energetic materials [22–24]. At present, many studies are being conducted on the flexibility and mechanical strength of polyurethane modified by HTPB at low temperatures and its application in related fields, but its application in the field of microfiber leather has rarely been studied [5,25,26].

In this paper, waterborne polyurethane was prepared using HTPB containing non-polar carbon as the soft segment, and the subsequent floating color washing efficiency was improved by reducing the binding fastness between WPU and the dispersed dye. Microfiber leather can thereby achieve better color binding upon rubbing after less washing times, reduce the discharge of dye sewage, and promote the development of the microfiber leather dyeing industry in the interests of environmental protection.

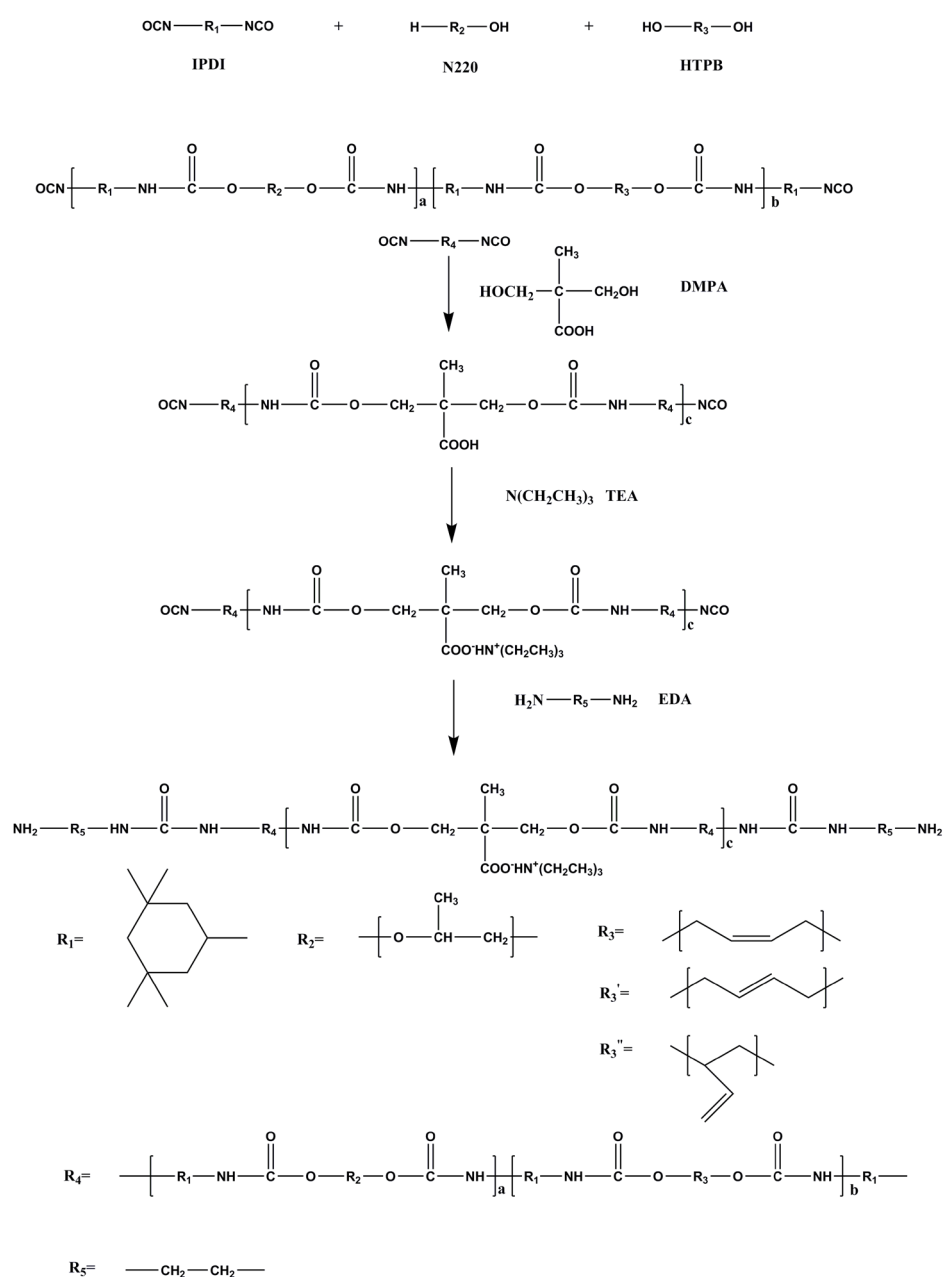
## 2. Materials and Methods

### 2.1. Materials

Poly(1,2-Propanediol) with a number molecular weight of 2000 (N220) was purchased from Zhongshan Chemical (Nanjing, China). It was dehydrated for 24 h at 110 °C under a vacuum prior to use. Industrial-grade isophorone diisocyanate (IPDI) was purchased from Bayer (Leverkusen, Germany). Hydroxyl-terminated polybutadiene was obtained from the LIMING Research Institute of Chemical Industry (Shenyang, China). Dimethylolpropionic acid (DMPA) was purchased from Baishun Chemical Reagent Co. Ltd. (Beijing, China). Trimethylamine (TEA) and ethylenediamine (EDA) were purchased from Fuchen Chemical Reagent Co. Ltd. (Tianjin, China).

## 2.2. Syntheses of HTPB-Modified Waterborne Polyurethane

Scheme 1 shows the WPU synthesis scheme while Table 1 represents the main components of the WPU samples.



**Scheme 1.** Syntheses of HTPB-modified waterborne polyurethane (H-WPU).

**Table 1.** The main compositions of the prepared waterborne polyurethane.

Samples	R	w(HTPB)/%	w(DMPA)%	Solid Content	HS/%
M1WPU-0	1.6	0	4	25	35
M1WPU-1	1.6	10	4	25	35
M1WPU-2	1.6	20	4	25	35
M1WPU-3	1.6	30	4	25	35
M1WPU-4	1.6	40	4	25	35
M1WPU-5	1.6	50	4	25	35
M1WPU-R1.3	1.3	10	4	25	35
M1WPU-R1.9	1.9	10	4	25	35
M1WPU-R2.2	2.2	10	4	25	35

w(HTPB)% is the percentage of added HTPB to the total content of HTPB and PPG, and w(DMPA)% is the percentage of DMPA to the total mass of the system.

Metered HTPB, PPG2000, and catalyst DBTDL were added to a 3-necked flask and stirred under nitrogen atmosphere, and the temperature was raised to 80 °C for 2 h. Subsequently, the heat was reduced to 60 °C, a certain amount of DMPA and metered butanone was added, the mixture was heated to 80 °C, and the reaction continued for 4 h. The mixture was cooled to 40 °C while the viscosity was adjusted with an appropriate amount of acetone. The metered TEA was added to neutralize the prepolymer. Finally, an aqueous polyurethane emulsion was obtained after emulsification with 200 g water and an appropriate amount of EDA at a speed of 3000 rpm.

### 2.3. Preparation of Microfiber Leather by Impregnating

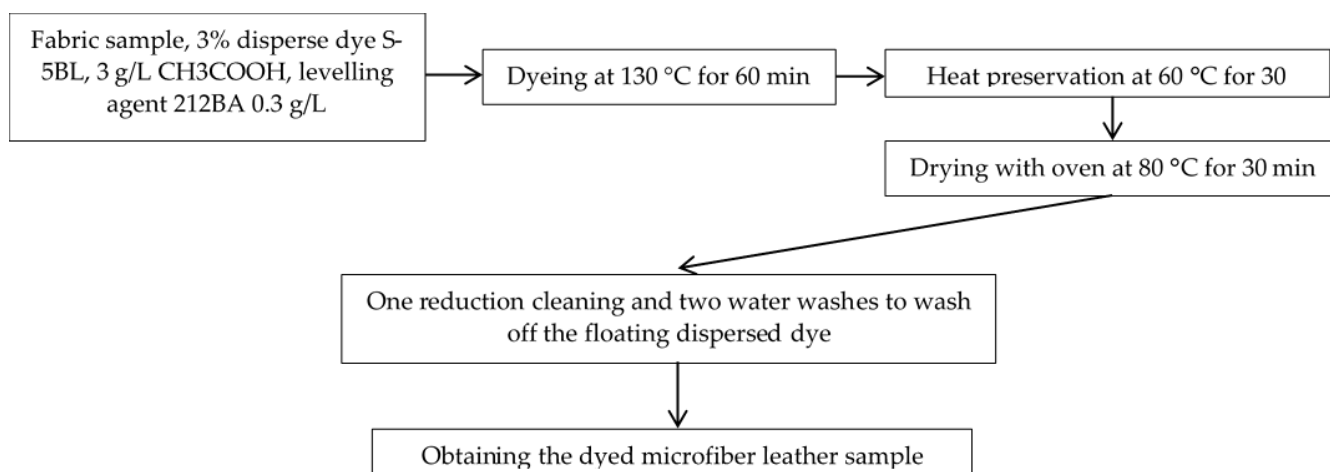
A specific method was used to impregnate the waterborne polyurethane into the non-woven fabrics to ensure that the wet slurry was adequately sampled on the microfiber base. During the impregnation, by adjusting the rolling pressure of the lower roll on the rolling cart, the uptake sample amount was controlled at 30%, to ensure the best performance for the microfiber leather products [1]. After impregnation, a huge drying oven was used to remove excess water and ensure the polyurethane resin cure was complete at the microfiber base with three-period drying so that the microfiber synthetic leather products met the standards.

Subsequently, alkali weight reduction was adopted to remove the sea structure from island fibers, and the concentration of alkali solution was configured at 10 g/L NaOH solution, using infrared 100 °C of 60 min for alkali weight reduction, and the infrared dye prototype was used to reduce the alkali content at 100 °C for 60 min. Then, the temperature was lowered to 60 °C to remove the products. The microfiber leather was then rinsed twice with warm water at 60 °C and then soaked in warm water at 60 °C, and 2 drops of 10% CH<sub>3</sub>COOH were added to the water for 10 min for neutralization. Finally, the residual alkaline lotion was rinsed with clean water, rolled once with a tandem roller, and dried in an oven at 80 °C for 30 min before it was removed.

### 2.4. Dyeing of Microfiber Leather with Dispersed Dye

The dyeing procedure was carried out according to Scheme 2. The initial temperature was 40 °C, and the heating rate was 1 °C/min.

The sample was dyed with red dispersed dye S-5BL. Firstly, the microfiber leather cloth sample was placed in the dyeing vat, and 3% (owf, on weight of fabric) dispersed dye was added. The dye vat bath ratio was cloth weight: dye liquor = 1:20, and 3 g/L CH<sub>3</sub>COOH was added to adjust the pH to 4.5–5.5, and 0.3 g/L drop leveling agent 212BA to ensure the dispersed dye fully bonded to the microfiber leather. Secondly, the microfiber leather was placed in the infrared dyeing machine, and the initial temperature was set to 40 °C, 1 °C/min for heating. The dye was dyed at a constant temperature of °C for 40 min, and then cooled to 60 °C for 30 min. Finally, the dyed microfiber leather was taken out and dried in an oven at 85 °C for 30 min.



**Scheme 2.** Dyeing process of microfiber leather.

The reduction cleaning solution was prepared with 6 g/L NaOH and 6 g/L sodium dithionite. Reductive cleaning was performed at 80 °C for 3 min, then cooled to 60 °C, and taken out and washed twice with water at the same temperature. The residual dye liquor concentration was characterized and analyzed with a UV spectrophotometer.

## 2.5. Characterization

### 2.5.1. Emulsion Particle Size and Zeta Potential Test

The particle size and zeta potential were evaluated using a Zetasizer Nana ZS90 (Malvern Instrument, Worcestershire, UK). The test emulsion was first diluted in deionized water to 0.01%, the temperature was set to 25 °C, and the results were averaged over 3 tests.

### 2.5.2. FTIR Spectrum

The FTIR spectra of the films were recorded using a Thermo Fisher Nicolet 8700 FTIR spectrophotometer (Thermo Fisher Scientific, Waltham, MA, USA). The tested sample was scanned 65 times at a resolution of 5 cm<sup>−1</sup>, with a scanning range of 700–5000 cm<sup>−1</sup>.

### 2.5.3. Contact Angle Test

The WPU's contact angle to water was characterized with a OCA20 type contact angle tester (Dataphysics Instrument, Stuttgart, German). The results were taken approximately 3 s after 2 µL of deionized water was added to the film. Five points were taken from each sample, and the average value was calculated.

### 2.5.4. Thermal Characterization

Differential scanning calorimetry (DSC) of the WPU films was performed with a METTLER DSC1 differential scanning calorimeter (Mettler Toledo, Zurich, Switzerland) with a 10 K/min heating rate in an N<sub>2</sub> atmosphere. Starting from room temperature, the sample was heated up to 150 °C at a rate of 10 K/min and held for 5 min, then cooled down to −100 °C at a rate of 10 K/min and held at −100 °C for 5 min, and, finally, heated up to 150 °C to complete the test.

Thermogravimetric analysis (TG) of the WPU films was performed with a METTLER TGA/DSC1 thermo gravimetric analyzer (Mettler Toledo, Zurich, Switzerland) with a 10 K/min heating rate in an N<sub>2</sub> atmosphere; the temperature started at 30 °C and ended at 500 °C. Weight loss was recorded as a function of the temperature.

### 2.5.5. Mechanical Characterization

The sample was cut into 20 mm × 4 mm dumbbell-shaped splines for testing, and the tensile rate was 10 mm/min. Each sample was cut into three splines for testing and

the average value was obtained. The experiment was carried out using a AGS-J electronic tensile testing machine (Shimadzu Corporation, Kyoto, Japan).

### 2.5.6. Scanning Electronic Microscopy

Scanning electronic microscopy (SEM) images of the microfiber synthetic leather were obtained from a Hitachi SU8020 microscope (Hitachi, Tokyo, Japan) with an accelerating voltage of 5.0 kV.

### 2.5.7. UV Characterization

The UV absorption spectrum was taken from a U-3900 UV-Vis Spectrophotometer (Hitachi, Tokyo, Japan), and the scanning wavelength range was set to 200 to 800 nm under a 1 nm resolution. The dispersed dye concentration was calculated according to Lambert–Beer’s law, and for dilute solutions, the absorbance was proportional to the concentration:

$$A = \lg (1/T) = Kbc$$

where A represents the absorbance, T is the transmittance, and K is the molar absorption coefficient, which is related to the properties of the absorbing material and the wavelength of the incident light. For b and c, b represents the thickness of the liquid layer while c is the concentration of the tested solution. If the wavelength of light is fixed, the absorption coefficient remains the same for the same substance.

## 3. Results and Discussion

### 3.1. The Emulsion Properties of HTPB-Modified Waterborne Polyurethane

The particle size and zeta potential of the HTPB-modified waterborne polyurethane are shown in Tables 2 and 3.

**Table 2.** Results of the particle size and the zeta potential for different HTPB contents.

Sample	Particle Size/nm	PDI	Zeta Potential/mV
M1WPU-0	74.8	0.084	−50.4
M1WPU-1	183.6	0.071	−41.3
M1WPU-2	188.8	0.089	−47.6
M1WPU-3	243.5	0.137	−38.6
M1WPU-4	267.0	0.340	−34.2
M1WPU-5	302.7	0.092	−31.4

**Table 3.** The results of the particle size and zeta potential for different R values.

Sample	Particle Size/nm	PDI	Zeta Potential/mV
M1WPU-R1.3	167.5	0.240	−47.7
M1WPU-R1.6	183.6	0.071	−41.3
M1WPU-R1.9	230.5	0.132	−33.8
M1WPU-R2.2	244.1	0.349	−29.9

From the perspective of the HTPB content, the emulsion particle size of the M1WPU-0 group without HTPB was about 74.8 nm, and the particle size increased to 183.6 nm when 10% HTPB was added. Moreover, with the increase in the HTPB content, the average particle size of the emulsion showed an increasing trend, the average particle size was above 150 nm, and the particle size distribution width gradually widened. Regarding the cause of the increases in the average particle size, although DMPA was added as a hydrophilic chain extender, after the introduction of HTPB into the polyether polyol system, because the HTPB molecules themselves also have long non-polar carbon chains, the hydrophilicity of the HTPB-modified waterborne polyurethane resin was greatly reduced. As a result, emulsification and dispersion of the prepolymer in water became more difficult,

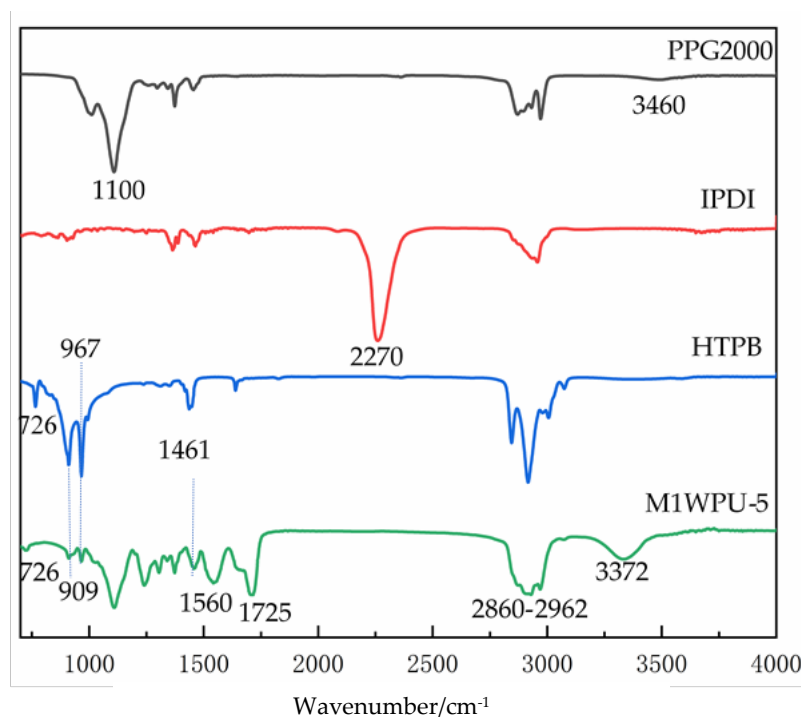
and the average particle size of the emulsion increased due to the difficulty in dispersing the prepolymer.

In addition, the HTPB molecule itself has three spatial conformations, namely, the 1, 4-homeopathy, 1, 4-trans, and 1, 3-butadiene structure. These three structures are shown in the reaction formula: R3, R3', and R3''. The existence of these three different spatial configurations results in large spatial steric hindrance inside the molecule, thus forming a large spatial structure of the molecule as a whole [22,27].

For different R values, the average particle size increased with the increase in the R value, from 167.5 to 244.1 nm. This was mainly due to the fact that in the process of post chain extension, when EDA was added for the post chain extension, the selected post-chain extension ratio was 0.8. As the R value increases, more -NCO groups remain on the surface of the prepolymer, thus forming a greater urea linkage area inside the WPU structure and making the formation of the electric double-layer structure more challenging. Consequently, the average particle size increases and the number of particles decreases.

### 3.2. FTIR Spectrum

Figure 1 shows the FTIR spectra of PPG2000, IPDI, HTPB, and HTPB-modified WPU.



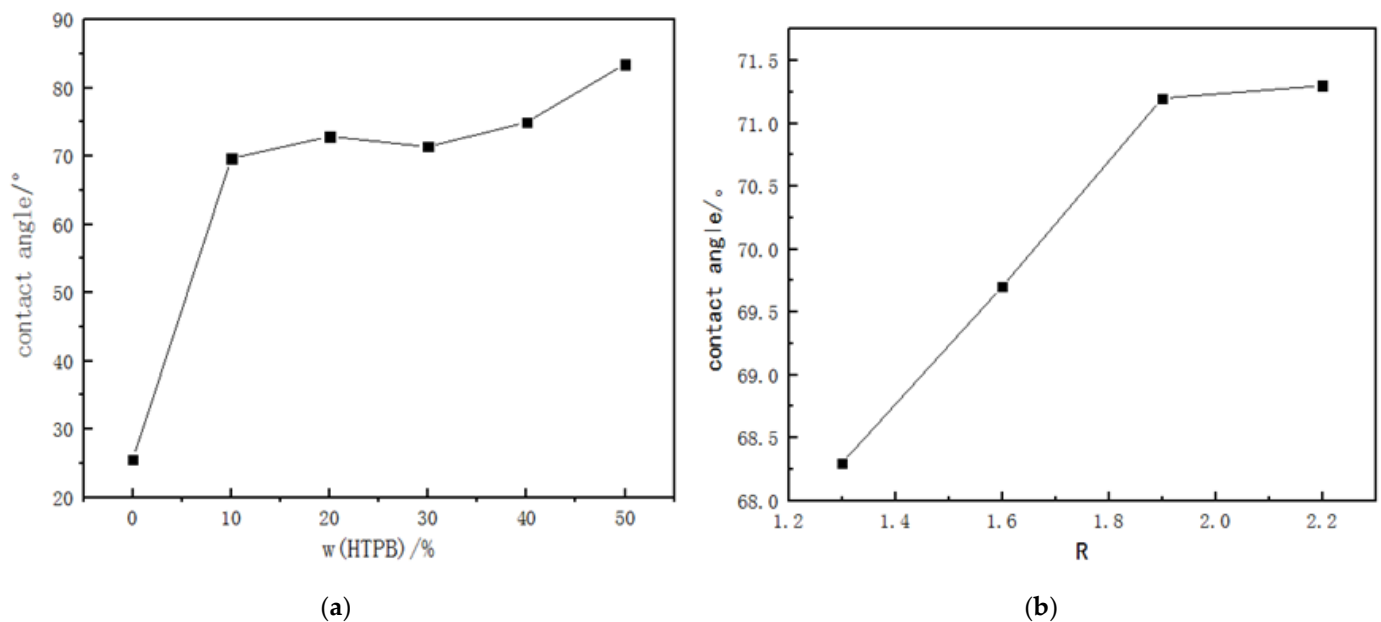
**Figure 1.** FTIR spectrum of PPG2000, HTPB, IPDI, and M1WPU5.

Figure 1 shows the FTIR spectrum results for the raw materials and WPU, which contained 50% HTPB. N220 has peaks at 1100 and 3460  $\text{cm}^{-1}$  for the absorption peaks of C-O-C and -OH, respectively. The modified waterborne polyurethane with different HTPB contents did not show the characteristic absorption peak of -NCO in the IPDI at 2270  $\text{cm}^{-1}$ , indicating that -NCO in the raw material fully participated in the reaction, and no IPDI was left. In the wavelength range from 2860 to 2962  $\text{cm}^{-1}$ , the stretching vibration absorption peaks of -CH<sub>3</sub>, -CH<sub>2</sub>, and -CH were, respectively, the carbonyl absorption peak on the carbamate bond formed by the reaction of -OH and -NCO at 1725  $\text{cm}^{-1}$ . The characteristic absorption peak of triethylamine carboxylate could be found at 1461  $\text{cm}^{-1}$  [28]. The stretching vibration absorption peak and bending vibration absorption peak of the N-H bond were at 3372 and 1560  $\text{cm}^{-1}$ . For the three carbon-carbon double bonds of HTPB, the three characteristic absorption peaks, located at 726, 967, and 909  $\text{cm}^{-1}$ , respectively, indicate the 1,4-homeopathy, 1,4-trans, and 1,3-butadiene structures of HTPB [7,21,23].



### 3.3. Hydrophilic Characterization of the HTPB-Modified Waterborne Polyurethane

The hydrophilic properties of M1WPU and M2WPU are shown in Figure 2. The contact angle of WPU without HTPB was  $25.6^\circ$ , which showed strong hydrophilicity. When the 10% HTPB content was added, the contact angle reached  $69.7^\circ$ , and the hydrophobicity increased significantly. With the increase in the HTPB content, the hydrophobicity of the WPU film gradually increased. This hydrophobic increase was mainly due to the long hydrophobic chain contained in the HTPB, which was introduced to the WPU, improving the whole hydrophobicity of the soft segment; on the other hand, due to the three kinds of conformation of HTPB, 1, 4-trans 1, 4-, and 1, 3 butadiene exist at the same time, and the three hydrophobic conformations in space form a hydrophobic space structure, further improving the film's degree of hydrophobicity [24,29].



**Figure 2.** Contact angle results of HTPB-modified WPU: (a) Contact angle of WPU with different HTPB contents; (b) Contact angle of WPU with different R values.

For different R values, as the R value increases, the contact angle increases slightly (compared with M1WPU) and the hydrophobicity becomes stronger, mainly due to the increase in the hard segment content. The increase in the hard segment quantity and density improves the degree of cross-linking. The improvement in this cross-linking structure makes the film form a dense cross-linking network, which can block the water molecules on its surface.

### 3.4. Thermal Properties

The differential scanning calorimetry (DSC) results for M1WPU-0 to M1WPU-5 are shown in Figure 3. The glass transition temperatures for WPU with different HTPB contents are shown in Table 4.

**Table 4.** Glass transition temperatures for M1WPU-1 to M1WPU-5.

Sample	M1WPU-0	M1WPU-1	M1WPU-2	M1WPU-3	M1WPU-4	M1WPU-5
T <sub>g</sub> , s/°C	−51.00	−53.33	−55.67	−56.67	−59.50	−61.83
T <sub>g</sub> , h/°C	111.33	117.17	119.33	119.83	120.00	121.67
ΔT <sub>g</sub>	162.33	170.50	175.00	176.5	179.5	189.5



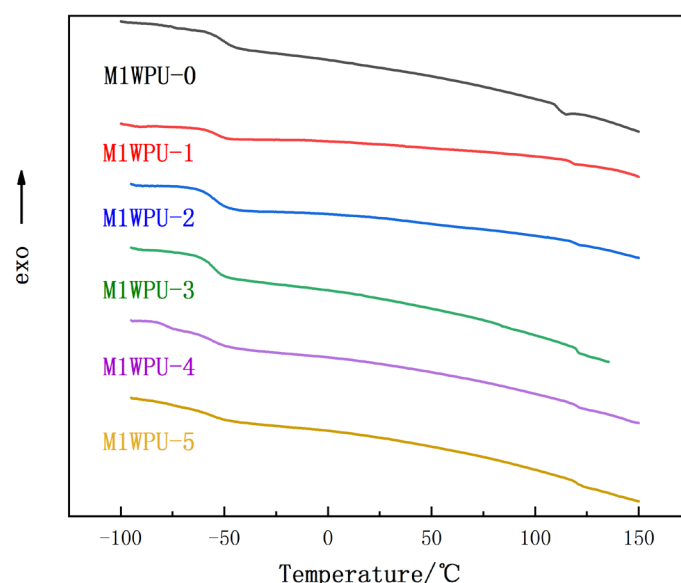


**Figure 3.** DSC result for M1WPU-0 to M1WPU-5.

As can be seen from Table 4, with the increases in the HTPB content, the glass transition temperature of the soft segment moves to low temperatures, while the glass transition temperature of the hard segment moves to high temperatures. The glass transition temperature difference between the hard and soft segments gradually increases, and the degree of microphase separation between the hard and soft segments increases noticeably.

This is mainly because the addition of HTPB adds some non-polar chain segments to the soft segment, which reduces the overall polarity of the soft segment, thus reducing the number of hydrogen bonds formed between the soft and hard segments and reducing the controlling effect of the hard segment on the soft segment. At low temperatures, the hard section, which easily crystallizes, cannot easily intervene in the crystallization process of the soft section, thus reducing the low-temperature glass transition temperature of the soft section and improving the low temperature flexibility of the modified WPU [24,25]. For the hard segment, due to the weakening of the binding strength of the soft segment, more hydrogen bonds are formed between the hard segments, and the degree of crystallization is strengthened. As a result, the glass transition temperature of the hard segment is increased, and the degree of separation of the hard segment is further increased.

Figure 4 shows the TG curve and DTG curve of the HTPB-modified waterborne polyurethane film. Table 5 shows the temperature and the final carbon residue of the modified water-based polyurethane film with different HTPB contents at a 5% weight loss and 50% weight loss.

It can be seen from Figure 4 that the decomposition of the HTPB-modified WPU film is mainly between 200 and 500 °C, and the temperature continues to rise after 500 °C; the residual carbon content is basically unchanged, indicating that the film is completely decomposed.

The film decomposition is divided into three stages: the first stage corresponds to 200~270 °C, which represents the decomposition of carboxylate (DMPA-TEA); the second stage corresponds to 270~350 °C, which represents the decomposition of urethane bonds; the third stage corresponds to 350~500 °C, which represents the decomposition of the soft segment PPG2000 and HTPB. For the decomposition of the soft segment, the modified WPU film with more than a 20% HTPB addition has a characteristic decomposition peak between 450 and 500 °C in the DTG curve. This stage represents the decomposition of HTPB. With the gradual increase in the HTPB content, the decomposition of the HTPB peaks became more pronounced and was correlated with increased HTPB enrichment [25].

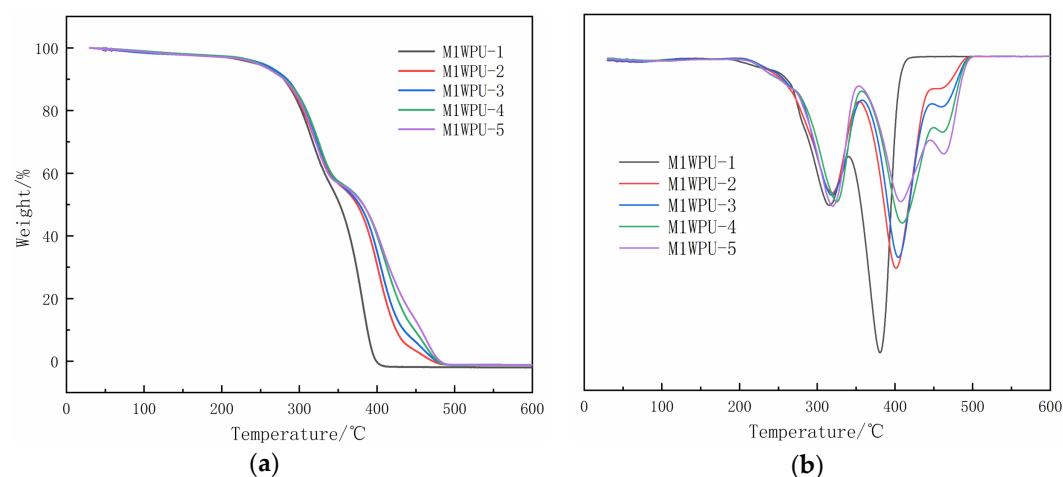


**Figure 4.** (a) TG and (b) DTG curves of HTPB-modified waterborne polyurethane.

**Table 5.** TG data of different HTPB-modified WPU films.

Sample	T5%/°C	T50%/°C	Residual Carbon/%
M1WPU-1	247	352	0.5
M1WPU-2	250	374	0.4
M1WPU-3	252	375	0.7
M1WPU-4	248	383	1.0
M1WPU-5	249	384	0.6

As shown in Table 6, with the increase in the HTPB content, the decomposition temperature of the 5% weight loss showed little change, but the decomposition temperature of the 50% weight loss increased. From 352.2 to 383.8 °C, the increase in the decomposition temperature of the 50% weight loss shows that the thermal stability of the film is improved when the HTPB modification is used to prepare WPU. There are two main reasons for this improvement in the thermal stability. First, the HTPB molecule contains a large amount of C=C, and the bond energy of the C=C double bond ( $606 \text{ KJ.mol}^{-1}$ ) is much higher than that of the C-C bond ( $332 \text{ KJ.mol}^{-1}$ ) and C-O ( $326 \text{ KJ.mol}^{-1}$ ) bond energies, so the destruction of the internal chemical bonds requires higher energy, and the overall thermal stability is improved. The C-H bond is easily attacked by oxygen atoms due to its small bond energy, forming highly reactive free radicals, and cross-linking reaction occurs between different free radicals during the WPU preparation reaction, thereby improving the overall thermal stability of the molecule.

**Table 6.** Alkali reduction ratio of M1WPU-0 to M1WPU-5.

Samples	M1WPU-0	M1WPU-1	M1WPU-2	M1WPU-3	M1WPU-4	M1WPU-5
Weight of nonwovens/g	16.00	16.00	16.00	16.00	16.00	16.00
Wet weight/g	32.74	32.68	31.46	32.08	32.06	31.88
Dry weight/g	20.98	20.75	21.04	21.03	20.89	20.68
Gain ratio/%	31.10	29.66	31.50	31.43	30.54	29.25
Weight after alkali reduction/g	15.59	15.45	15.76	15.84	15.76	15.36
Alkali reduction ratio/%	33.67	33.12	32.99	32.45	32.01	33.27

### 3.5. Mechanical Properties of WPU Films

The results of the characterization of the mechanical properties of the WPU film are shown in Figure 5.

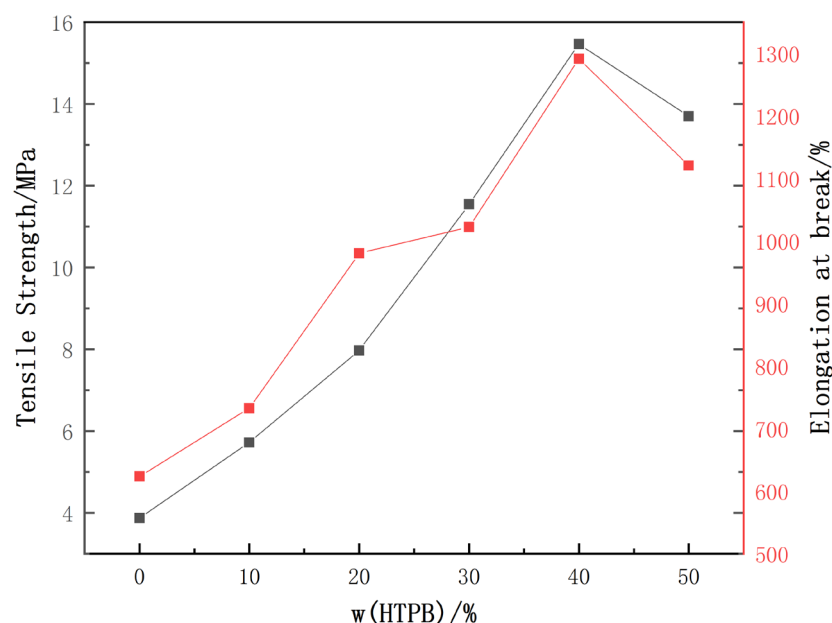


**Figure 5.** Mechanical properties of waterborne polyurethane films with different HTPB contents.

It can be seen from Figure 5 that with the addition of HTPB from 0% to 50%, the maximum tensile strength and elongation at break of the WPU film first increased and then decreased, and the maximum tensile strength appeared for the 40% HTPB additions. At this time, the elongation at break was 882.6%, which is 87.5% higher than that of WPU without HTPB. The maximum tensile strength is 159.5% higher than that of WPU without HTPB. The introduction of HTPB can improve the mechanical properties of the WPU film to a certain extent.

An analysis of the reasons shows that the HTPB molecule contains a long non-polar hydrophobic carbon chain, which leads to microphase separation between the soft and hard segments of WPU itself, and the degree of separation increases with the increase in HTPB. Proper microphase separation weakens the binding of the hard segment to the soft segment to a certain extent, so that the hard segment moves to the middle of the soft segment as a kind of physical cross-linking point [28]. While the HTPB content increased to 50%, the tensile strength decreased from 15.3 to 13.9 MPa, and the elongation at break decreased from 1315% to 1123% due to excessive microphase separation.

### 3.6. Alkali Reduction Ratio of Microfiber Synthetic Leather

The alkali reduction results of the modified microfiber leather are shown in Table 6.

After the alkali reduction, it was found that the alkali reduction of the HTPB-modified WPU emulsion after impregnation on the non-woven fabric was lower than that of the unmodified WPU emulsion. After the water-based polyurethane resin was impregnated, the alkali reduction process occurred not only due to a reduction in the sea-island fiber part of the non-woven fabric but also a reduction in the water-based polyurethane. The alkali reduction rate after the final impregnation was about 30%. With the increase in the HTPB content, the alkali reduction rate showed a decreasing trend, indicating that the introduction of HTPB into the original WPU system could improve the alkali resistance of resin components. This is mainly due to the fact that the final step of microfiber leather preparation was as high as 160 °C, and high temperatures promote the cross-linking of HTPB double bonds, thereby increasing the cross-linking density of water-based polyurethane [25], and hindering the penetration of hydroxide corrosive ions; on the other hand, in the process of synthesizing WPU, the selected PPG 2000 was a polyether polyol, and its alkali resistance was better than that of polyester polyol.

The decrease in the alkali reduction rate improved the quality of the final microfiber product, indicating that more modified WPU can be impregnated into the microfiber-based

fabric system, increasing the amount of modified waterborne polyurethane loaded, and reducing the number of washes.

However, when the HTPB content was higher than 40%, the alkali reduction rate tended to increase. This may be because the addition of an excess of non-polar polymer chains reduced the hydrogen bonding of the soft and hard segments, resulting in further aggravation of the microphase separation of the soft and hard segments. The microdomain structure between the segments is destroyed and can no longer effectively block the penetration of corrosive ions in the alkali solution, which aggravates the degradation of the polyurethane component during the alkali reduction process, resulting in an increase in the alkali reduction rate.

The *t*-Test results of the alkali reduction ratio are shown in the Supplementary Materials, which prove that the alkali reduction ratio values have statistical validity.

The SEM characterization results of the microfiber leather structure after alkali reduction are also shown in the Supplementary Materials.

### 3.7. Ultraviolet Spectral Characterization of Floating Color of Microfiber Leather

The microfiber synthetic leather impregnated with different polyurethane components was dyed with dispersed red S-5BL. After dyeing, 6 g/L safety powder and 6 g/L NaOH were used to prepare the reduction cleaning solution. Reduction cleaning was carried out at 80 °C for 30 min. After washing, it was taken out and washed with clean water for the second and third time. Subsequently, UV spectrophotometry was used to show the UV test results of the retained reduction cleaning solution. According to Lambert–Beer’s law:

$$A = \lg(1/T) = Kbc$$

The standard curve of the dispersed S-5BL dye is shown in the Supplementary Materials.

Figure 6 shows the UV results of the residual solution after three washes of microfiber synthetic leather dyed with dispersed S-5BL dye.

By comparing the results of the third washing curve, the maximum absorption wavelength of the dispersed red S-5BL solution was determined to be 510 nm. For the peaks at about 300 nm, the benzene ring and unsaturated conjugated olefin may have taken part in these peaks, because these structures have a strong characteristic absorption peak at 250–300 nm. The maximum absorbance corresponding to the peak value was substituted into the standard equation; therefore, the concentration of dispersed S-5BL dye in the relevant solution was calculated. According to the corresponding Lambert–Beer’s law, all liquid samples were diluted to a suitable concentration between 0.2 and 0.9, where  $\delta C$  is the concentration difference compared to that of the microfiber leather impregnated by unmodified WPU. The calculated results are shown in Tables 7–10.

**Table 7.** Concentration of residual dye after the first reduction cleaning.

HTPB Content/%	0	10	20	30	40	50
Absorbance (A)	0.258	0.318	0.356	0.451	0.560	0.621
Concentration/mg·L <sup>−1</sup>	70.92	87.42	97.86	123.99	153.94	170.77
Dilution ratio	10	10	10	10	10	10
Concentration after adjustment/mg·L <sup>−1</sup>	709.20	874.20	978.60	1239.90	1539.40	1707.70
$\delta C$ /%	0.00	23.25	37.98	74.80	117.05	140.69

**Table 8.** Concentration of residual dye after the second wash.

HTPB Content/%	0	10	20	30	40	50
Absorbance (A)	0.581	0.562	0.464	0.395	0.253	0.187
Concentration/mg·L <sup>−1</sup>	159.72	154.56	127.55	108.68	69.55	51.43
Dilution ratio	4	4	4	4	4	4
Concentration after adjustment/mg·L <sup>−1</sup>	638.88	618.24	510.20	434.72	278.20	205.72
$\delta C$ /%	0.00	−3.27	−20.14	−32.01	−56.45	−67.81

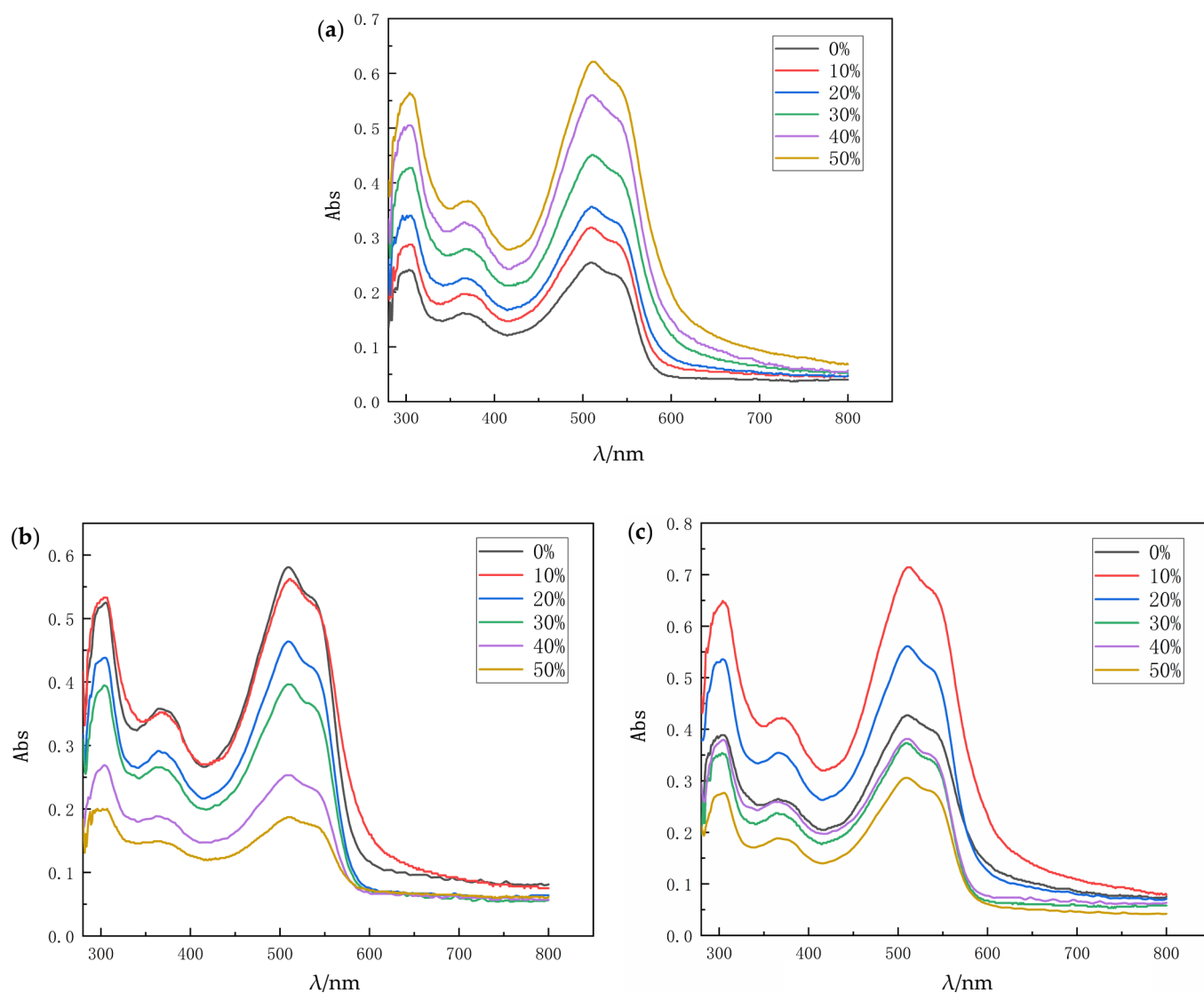


**Figure 6.** UV results of the residual dye: (a) after the first wash; (b) after the second wash; (c) after the third wash.

**Table 9.** Concentration of residual dye after the third wash.

HTPB Content/%	0	10	20	30	40	50
Absorbance (A)	0.427	0.714	0.562	0.373	0.380	0.306
Concentration/ $\text{mg}\cdot\text{L}^{-1}$	117.42	196.37	154.51	102.55	104.45	84.17
Dilution ratio	4	2	2	2	0	0
Concentration after adjustment/ $\text{mg}\cdot\text{L}^{-1}$	469.68	392.74	309.02	205.10	104.45	84.17
$\delta C/\%$	0.00	−16.40	−34.19	−56.33	−77.75	−82.09

**Table 10.** Concentration of residual dye after the third wash.

HTPB Content/%	0	10	20	30	40	50
Concentration after the first wash/ $\text{mg}\cdot\text{L}^{-1}$	709.20	874.20	978.60	1239.90	1539.40	1707.70
Concentration after the first wash/ $\text{mg}\cdot\text{L}^{-1}$	638.88	618.24	510.20	434.72	278.20	205.72
Concentration after the first wash/ $\text{mg}\cdot\text{L}^{-1}$	469.68	392.74	309.02	205.10	104.45	84.17
Decoloration rate/%	13.18	25.54	37.24	55.05	74.66	81.27

HTPB content represents the content of HTPB in the water-based polyurethane impregnated for the microfiber leather.

In order to better characterize the decolorization efficiency, the decoloration rate was introduced. The decoloration rate can be calculated by the following formula:

$$\text{decoloration rate} = \frac{C_1 - C_3}{C_1 + C_2 + C_3}$$

where  $C_1$ ,  $C_2$ , and  $C_3$  represent the dye concentration after the first, second, and third water wash, respectively. The decoloration rate reflects the level of elution efficiency, where a higher decoloration rate indicates that more floating dye is washed away by the first wash rather than subsequent wash steps.







From three washes, the first reduction cleaning washed away most of the floating dye. Compared with the unmodified leather, the amount of floating color removed by the first wash after dyeing increased by 23.25%, 37.98%, 74.80%, 117.05%, and 140.69%, respectively, indicating that the addition of HTPB reduced the combination of dye and impregnated water-based polyurethane, thereby improving the efficiency of floating color cleaning. For the microfiber leather prepared by impregnation with unmodified water-based polyurethane, the decoloration rate was about 13.18%, while the microfiber leather prepared by 50% HTPB-modified waterborne polyurethane reached 81.27%. The floating efficiency was greatly improved.

The main reason is that in the modified waterborne polyurethane with a higher HTPB content, more non-polar carbon chains were introduced into the waterborne polyurethane system during the synthesis process, which reduced the overall polarity of the resin structure. There are few polar groups in the main chain of the HTPB molecule, and the overall structure is in a low polarity state. Therefore, in the dyeing process, the intermolecular force and hydrogen bond that formed with the dispersed dye are weak. Dispersed dyes have strong hydrophobicity, low solubility in water, and a lack of water-soluble groups in their structure. The introduction of HTPB will weaken the bonding strength between the dispersed dye and modified water-based polyurethane, making it easier for the dispersed dye easier to be eluted after dyeing and allowing better color binding to be achieved with fewer washes.





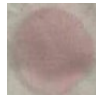
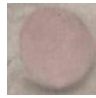
### 3.8. Color Binding upon Rubbing of the HTPB-Modified Microfiber Leather

Tables 11 and 12 show the results of the color fastness regarding the rubbing of HTPB-modified microfiber leather after three washes.

**Table 11.** Color binding upon dry rubbing of the modified microfiber leather.

HTPB Content/%	0	10	20	30	40	50
Color fastness to dry rubbing						
grade	1–2	1–2	2	2–3	4	4–5

**Table 12.** Color binding upon wet rubbing of the modified microfiber leather.

HTPB Content/%	0	10	20	30	40	50
Color fastness to wet rubbing						
grade	1	1–2	1–2	1–2	3–4	3–4

HTPB content represents the content of HTPB in the water-based polyurethane impregnated in the microfiber leather.



The microfiber has a large specific surface area, so it has a strong adsorption capacity for dispersed dye. However, due to the saturation of the adsorption of dye on the fibers, many dyes do not fully enter the fiber during the adsorption process but are mechanically bound to the surface of the microfiber leather, resulting in poor color binding. On the other hand, for water-based polyurethane, dispersed dye mostly exists in the microporous structure of polyurethane in the form of single molecules, dye aggregates or dye crystals, and van der Waals force and hydrogen bonds combined with polyurethane, since the degree of van der Waals force and hydrogen bonding is much lower than the covalent bond strength. The poor interaction force between polyurethane and dye is also another important reason for poor color binding upon rubbing.

The results of the color binding upon rubbing show that for dispersed red S-5BL, with the increasing HTPB content, the color binding upon dry and wet rubbing of the corresponding microfiber leather products was improved, which was consistent with the maximum UV resistance of the residual dye solution during the process of water decolorization. As the bonding strength of water-based polyurethane and dispersed dye was weakened, the amount of floating dye remaining in the HTPB-modified microfiber leather after three washes was greatly reduced, and, thus, the color binding upon rubbing was improved accordingly. For the dispersed dye S-5BL, the grade of binding upon dry rubbing increased from 1–2 to 4–5, and the grade of binding upon wet rubbing increased from 1 to 3–4. The grade of the color binding upon rubbing meets the relevant application requirements.

#### 4. Conclusions

For the first time, HTPB was used in this study to improve the color binding of microfiber leather. The addition of HTPB increased the average particle size of polyurethane emulsions and worsened the storage stability and centrifugal stability. Because HTPB molecules have longer hydrophobic carbon chains, which improves the hydrophobicity of modified waterborne polyurethane, the emulsification process of waterborne polyurethane becomes more difficult, and larger particles are formed after emulsification. From the perspective of the spatial structure, HTPB molecules also have three hydrophobic conformations due to their spatial hydrophobic structure in space: 1,4-homeopathic, 1,4-trans, and 1,3-butadiene conformations, which further improves the hydrophobic efficiency of waterborne polyurethane film.

The DSC and TG results mainly showed that with the increase in the addition of HTPB, the degree of microphase separation between the hard and soft segments of waterborne polyurethane increased. The glass transition temperature difference between the soft and hard segments showed an increasing trend.

The modified microfiber leather was prepared by impregnating the HTPB-modified water-based polyurethane on the microfiber and dyeing it. The UV spectrum results showed that the decoloration rate of the microfiber leather modified by the 50% HTPB addition reached 81.27%, compared with 13.18% of the unmodified microfiber leather, and an increase of 68.09% was obtained. Combined with the results of the color binding upon rubbing, color binding in the context of dry and wet rubbing of microfiber leather prepared with 50% HTPB-modified waterborne polyurethane reached grades 4–5 and 3–4, respectively, compared with color binding on unmodified microfiber leather. The floating color washing efficiency was therefore significantly improved.

**Supplementary Materials:** The following are available online at <https://www.mdpi.com/article/10.3390/coatings12060728/s1>, Figure S1. SEM images for microfiber synthetic leather: (a) 0% HTPB content; (b) 10% HTPB content; (c) 20% HTPB content; (d) 30% HTPB content; (e) 40% HTPB content; (f) 50% HTPB content. Figure S2. Standard curve of disperse dye S-5BL. Table S1. UV absorbance of standard solutions with different S-5BL dispersed red content. Table S2. Regression equation parameters of S-5BL disperse dye. Table S3. Regression equation parameters of S-5BL disperse dye. Table S4. *t*-test results for alkali reduction.



**Author Contributions:** Conceptualization, W.X. and Y.L.; methodology, W.C.; validation, H.Z. and Y.L.; formal analysis, W.C.; resources, Y.L.; data curation, W.C. and H.Z.; writing—original draft preparation, W.C.; writing—review and editing, W.X. and Y.L.; supervision, H.Z.; project administration, W.X. and Y.L. All authors have read and agreed to the published version of the manuscript.

**Funding:** This research received no external funding.

**Institutional Review Board Statement:** Not applicable.

**Informed Consent Statement:** Not applicable.

**Data Availability Statement:** Not applicable.

**Conflicts of Interest:** The authors declare no conflict of interest.

## References

1. Sudha, T.B.; Thanikaivelan, P.; Aaron, K.P.; Krishnaraj, K.; Chandrasekaran, B. Comfort, chemical, mechanical, and structural properties of natural and synthetic leathers used for apparel. *J. Appl. Polym. Sci.* **2009**, *114*, 1761–1767. [\[CrossRef\]](#)
2. Liu, R.; Chen, Y.; Fan, H. Design, characterization, dyeing properties, and application of acid-dyeable polyurethane in the manufacture of microfiber synthetic leather. *Fibers Polym.* **2015**, *16*, 1970–1980. [\[CrossRef\]](#)
3. Qiang, T.; Wang, X.; Wang, X.; Ren, L.; Guo, P. Study on the improvement of water vapor permeability and moisture absorption of microfiber synthetic leather base by collagen. *Text. Res. J.* **2014**, *85*, 1394–1403. [\[CrossRef\]](#)
4. Li, Y.; Joo, C.W. Structural factors and physical properties of needle-punched nonwovens based on Co-PET/PA bicomponent fibers via alkali treatment. *Fibers Polym.* **2012**, *13*, 456–465. [\[CrossRef\]](#)
5. Hu, X.-h.; Liu, X.; Liu, M.-l.; Li, G. A waterborne polyurethane-based polymeric dye with covalently linked disperse red 11. *React. Funct. Polym.* **2018**, *132*, 1–8. [\[CrossRef\]](#)
6. Wang, Y.; Jin, L. Preparation and Characterization of Self-Colored Waterborne Polyurethane and Its Application in Eco-Friendly Manufacturing of Microfiber Synthetic Leather Base. *Polymer* **2018**, *10*, 289. [\[CrossRef\]](#)
7. Min Huang, S.; Ko Chen, T. Effects of ion group content and polyol molecular weight on physical properties of HTPB-based waterborne poly(urethane-urea)s. *J. Appl. Polym. Sci.* **2007**, *105*, 3796–3801. [\[CrossRef\]](#)
8. Dai, M.; Wang, J.; Zhang, Y. Improving water resistance of waterborne polyurethane coating with high transparency and good mechanical properties. *Colloids Surf. A Physicochem. Eng. Asp.* **2020**, *601*, 124994. [\[CrossRef\]](#)
9. Amrollahi, M.; Sadeghi, G.M.M. Assessment of adhesion and surface properties of polyurethane coatings based on non-polar and hydrophobic soft segment. *Prog. Org. Coat.* **2016**, *93*, 23–33. [\[CrossRef\]](#)
10. Akram, N.; Zia, K.M.; Saeed, M.; Usman, M.; Khan, W.G.; Bashir, M.A. Investigation of non-adhesive behaviour of waterborne polyurethane dispersions. *J. Polym. Res.* **2019**, *26*, 45. [\[CrossRef\]](#)
11. Zhou, X.; Fang, C.; Lei, W.; Su, J.; Li, L.; Li, Y. Thermal and Crystalline Properties of Waterborne Polyurethane by in situ water reaction process and the potential application as biomaterial. *Prog. Org. Coat.* **2017**, *104*, 1–10. [\[CrossRef\]](#)
12. Fu, Z.; Xu, M.; Sheng, Y.; Yan, Z.; Meng, J.; Tong, C.; Li, D.; Wan, Z.; Ming, Y.; Mei, A.; et al. Encapsulation of Printable Mesoscopic Perovskite Solar Cells Enables High Temperature and Long-Term Outdoor Stability. *Adv. Funct. Mater.* **2019**, *29*, 1809129. [\[CrossRef\]](#)
13. Bonomo, M.; Taheri, B.; Bonandini, L.; Castro-Hermosa, S.; Brown, T.M.; Zanetti, M.; Menozzi, A.; Barolo, C.; Brunetti, F. Thermosetting Polyurethane Resins as Low-Cost, Easily Scalable, and Effective Oxygen and Moisture Barriers for Perovskite Solar Cells. *ACS Appl. Mater. Interfaces* **2020**, *12*, 54862–54875. [\[CrossRef\]](#) [\[PubMed\]](#)
14. Wu, J.; Wang, C.; Lin, W.; Ngai, T. A facile and effective approach for the synthesis of fluorinated waterborne polyurethanes with good hydrophobicity and antifouling properties. *Prog. Org. Coat.* **2021**, *159*, 106405. [\[CrossRef\]](#)
15. Liu, C.; Yin, Q.; Li, X.; Hao, L.; Zhang, W.; Bao, Y.; Ma, J. A waterborne polyurethane-based leather finishing agent with excellent room temperature self-healing properties and wear-resistance. *Adv. Compos. Hybrid Mater.* **2021**, *4*, 138–149. [\[CrossRef\]](#)
16. Luo, H.; Liu, Y.; Ruj, B.; Sun, L.; Wang, J.; He, Y. Preparation of degradable castor oil-based waterborne polyurethane with tannic acid as crosslinking agent and its application on leather surface coating. *J. Polym. Anal. Character.* **2021**, *27*, 52–70. [\[CrossRef\]](#)
17. Wu, J.; Chen, D. Synthesis and characterization of waterborne polyurethane based on covalently bound dimethylol propionic acid to ε-caprolactone based polyester polyol. *Prog. Org. Coat.* **2016**, *97*, 203–209. [\[CrossRef\]](#)
18. Hussain, I.; Sanglard, M.; Bridson, J.H.; Parker, K. Preparation and physicochemical characterisation of polyurethane foams prepared using hydroxybutylated condensed tannins as a polyol source. *Ind. Crops Prod.* **2020**, *154*, 112636. [\[CrossRef\]](#)
19. Guilleme, S.M.; Khalil, H.; Misra, M. Green and sustainable polyurethanes for advanced applications. *J. Appl. Polym. Sci.* **2017**, *134*, 45113. [\[CrossRef\]](#)
20. Luo, Y.L.; Miao, Y.; Xu, F. Synthesis, phase behavior, and simulated in vitro degradation of novel HTPB-b-PEG polyurethane copolymers. *Macromol. Res.* **2011**, *19*, 1233–1241. [\[CrossRef\]](#)
21. Ge, Y.H.; Kang, J.Y.; Zhou, J.H.; Shi, L.W. Theoretical investigation on thermal aging mechanism and the aging effect on mechanical properties of HTPB-IPDI polyurethane. *Comput. Mater. Sci.* **2016**, *115*, 92–98. [\[CrossRef\]](#)

22. Poussard, L.; Burel, F.; Couvercelle, J.-P.; Loutelier-Bourhis, C.; Bunel, C. Synthesis of new anionic HTPB-based polyurethane elastomers: Aqueous dispersion and physical properties. *J. Appl. Polym. Sci.* **2006**, *100*, 3312–3322. [[CrossRef](#)]
23. Mingjie, H.; Wei, F.; Le, G.; Weibing, W.; Xinghai, L.; Chi, H. One-pot synthesis of hyperbranched polyols and their effects as crosslinkers on HTPB-based polyurethane. *Polym. Bull.* **2014**, *71*, 2671–2693. [[CrossRef](#)]
24. Malkappa, K.; Rao, B.N.; Jana, T. Functionalized polybutadiene diol based hydrophobic, water dispersible polyurethane nanocomposites: Role of organo-clay structure. *Polymer* **2016**, *99*, 404–416. [[CrossRef](#)]
25. Chen, C.J.; Tseng, I.H.; Lu, H.T.; Tseng, W.Y.; Tsai, M.-H.; Huang, S.-L. Thermal and tensile properties of HTPB-based PU with PVC blends. *Mater. Sci. Eng. A* **2011**, *528*, 4917–4923. [[CrossRef](#)]
26. Cao, Z.; Zhou, Q.; Jie, S.; Li, B.G. High cis-1,4 Hydroxyl-Terminated Polybutadiene-Based Polyurethanes with Extremely Low Glass Transition Temperature and Excellent Mechanical Properties. *Ind. Eng. Chem. Res.* **2016**, *55*, 1582–1589. [[CrossRef](#)]
27. Akram, N.; Gurney, R.S.; Zuber, M.; Ishaq, M.; Keddie, J.L. Influence of Polyol Molecular Weight and Type on the Tack and Peel Properties of Waterborne Polyurethane Pressure-Sensitive Adhesives. *Macromol. React. Eng.* **2013**, *7*, 493–503. [[CrossRef](#)]
28. Pérez-Limiñana, M.A.; Arán-Aís, F.; Torró-Palau, A.M.; César Orgilés-Barceló, A.; Miguel Martín-Martínez, J. Characterization of waterborne polyurethane adhesives containing different amounts of ionic groups. *Int. J. Adhes. Adhes.* **2005**, *25*, 507–517. [[CrossRef](#)]
29. Toosi, F.S.; Shahidzadeh, M.; Ramezanzadeh, B. An investigation of the effects of pre-polymer functionality on the curing behavior and mechanical properties of HTPB-based polyurethane. *J. Ind. Eng. Chem.* **2015**, *24*, 166–173. [[CrossRef](#)]